Article

The Impact of Dam Construction on Downstream Vegetation Area in Dry Areas Using Satellite Remote Sensing: A Case Study

Raid Almalki [1,2], Mehdi Khaki [3,*], Patricia M. Saco [3] and Jose F. Rodriguez [3]

1 School of Environmental and Life Science, University of Newcastle, Callaghan, NSW 2308, Australia; raidhassanh.almalki@uon.edu.au

2 Department of Geography, Umm Al-Qura University, Makkah 21955, Saudi Arabia

3 School of Engineering, University of Newcastle, Callaghan, NSW 2308, Australia; patricia.saco@newcastle.edu.au (P.M.S.); jose.rodriguez@newcastle.edu.au (J.F.R.)

* Correspondence: mehdi.khaki@newcastle.edu.au

Abstract: The assessment of ecosystem quality and the maintenance of optimal ecosystem function require understanding vegetation area dynamics and their relationship with climate variables. This study aims to detect vegetation area changes downstream of the Hali dam, which was built in 2009, and to understand the influence of the dam as well as climatic variables on the region's vegetation areas from 2000 to 2020. The case study is located in an arid area with an average rainfall amount from 50 to 100 mm/year. An analysis of seasonal changes in vegetation areas was conducted using the Normalized Difference Vegetation Index (NDVI), and supervised image classification was used to evaluate changes in vegetation areas using Landsat imagery. Pearson correlation and multivariate linear regression were used to assess the response of local vegetation areas to both hydrologic changes due to dam construction and climate variability. The NDVI analysis revealed a considerable vegetation decline after the dam construction in the dry season. This is primarily associated with the impoundment of seasonal water by the dam and the increase in cropland areas due to dam irrigation. A significantly stronger correlation between vegetation changes and precipitation and temperature variations was observed before the dam construction. Furthermore, multivariant linear regression was used to evaluate the variations in equivalent water thickness (EWT), climate data, and NDVI before and after the dam construction. The results suggested that 85 percent of the variability in the mean NDVI was driven by climate variables and EWT before the dam construction. On the other hand, it was found that only 42 percent of the variations in the NDVI were driven by climate variables and EWT from 2010 to 2020 for both dry and wet seasons.

Keywords: vegetation areas; dam impacts; downstream vegetation; climate variability; arid regions

1. Introduction

The scarcity of water and recurrent droughts in arid regions pose significant challenges to ecosystems and human communities [1]. These conditions often result in reduced water availability, impacting vegetation growth and survival [2]. Vegetation is one of the most fundamental parts of the earth's ecosystem [3,4]. Quantitative measurements of vegetation areas on well-defined spatiotemporal scales are important for ecological and climatological studies [5,6]. The Normalized Difference Vegetation Index (NDVI) is an indicator of vegetation's ability to absorb photosynthetically active radiation and is the most widely used vegetation index for analyzing vegetation dynamics [7]. The index measures the reflectance of vegetation in the red and near-infrared bands [8,9]. It is applied primarily in both global and regional studies to understand and quantify the impact of climate variables on vegetation productivity, phenology, and how vegetation responds to other factors and stressors [10,11]. Studying vegetation area changes over arid and semi-arid regions,

however, is very challenging. The vegetation areas in these regions are widely recognized as complex systems due to water stress, and its low density and sparse distribution [12]. Plant growth is limited in arid regions by a lack of precipitation and humidity combined with relatively high temperatures and evapotranspiration, which is sometimes highly dependent on global and local climates [13–16].

Many studies have shown the complexity of studying NDVI changes and their relationships with climate variabilities over semi-arid and arid regions [17–19]. Wang et al. [7] investigated the correlation between NDVI and temperature and precipitation in the central United States Great Plain. A high correlation was found between NDVI values during the growing season (March–October) and precipitation. Early and late in the growing season, NDVI correlated positively with temperature; however, in the middle, it correlated negatively [7]. A study by Xie et al. [20] found that temperature positively correlates with vegetation in most periods in semi-arid areas. In the Xinjiang desert of northwest China, vegetation has primarily shown a greening curve in recent decades, and the primary variable driving this process, as identified, is precipitation [21,22]. Tong et al. [23] mentioned that NDVI correlated positively with precipitation and temperature in the Inner Mongolian desert, where precipitation has a more substantial effect on vegetation variation than temperature.

Moreover, the impact of large dams can pose further difficulties to studying vegetation variation in dry areas by disrupting the water runoff downstream. Various studies have indicated different connections between local climate change and dam construction through analyses of precipitation and temperature changes. According to Degu et al. [24], large dams in Mediterranean climates have the most significant effect on the climate closer to reservoir areas and negligible influence in humid subtropical climates. Based on the study results, Zhao et al. [25] concluded that the reservoir in the Miyun area, with a catchment area of approximately 15,788 km^2, had a notable influence on both local temperature and precipitation during the summer months. A study by Chen [26] found that, while downstream precipitation had not changed significantly, the temperature increased following the impoundment of the Three Gorges Reservoir (with a catchment area around 1 million km^2) where is situated in China. Over the same region, Miller et al. [27], using multiple experiments to simulate the effects of the Three Gorges Reservoir on the local climate, found no effects on precipitation. But, a different study by Wu et al. [28] found that there is an effect on precipitation at the regional scale of 100 km rather than at the local scale. In the context of dam reservoirs situated in the southwestern region of Saudi Arabia, such as the Baish dam, the recorded figures for surface evaporation indicated a yearly range of 4.7–6.0 m [29]. Missimer et al. [29] also noted that, particularly in older stream systems, as much as 80% of water could be lost due to evaporation. The anticipated rise in temperature is expected to amplify evaporation losses from dam reservoirs, consequently impacting water resources [30].

Geographic information systems (GIS) and remote sensing have been used to study vegetation areas' changes and the corresponding impact of local climate variabilities. GIS and remote sensing provide essential data and tools for spatiotemporal detection modeling at a local and global scale for the past, present, and future. Several changes in vegetation can be detected and monitored through remote sensing, including changes in aboveground production, structure, and cover [31]. Vegetation areas change detection is critical for understanding the interaction and interrelationships of the ecosystem, climate, and human activities. Monitoring vegetation changes at different spatial and temporal scales using this technique is also important for detecting changes in vegetation structure, function, and interaction with climate variabilities [32,33].

Previous studies have investigated the NDVI and climate variables using various variables such as sunshine, wind velocity, and direction, allowing them to measure the NDVI's determinants with good precision [34]. Nevertheless, temperature and precipitation have been found to be the two most used [34]. Srivastava et al. [35] investigated semi-arid dryland areas in six districts in India, and they found that the NDVI has a much

stronger relationship with the amount of water consumed by vegetation than precipitation. Moreover, a study by Ji and Peters [36], which used six climate variables to analyze the grasslands of the United States' Great Plains, water condition was the most important factor in determining vegetation growth. In addition, in an effort to comprehend the shifts in the hydrological cycle through the application of remote sensing technology, accessible observations of Total Water Storage (TWS) primarily pertained to the timeframe encompassed by the Gravity Recovery and Climate Experiment (GRACE) mission. Tangdamrongsub et al. [37] meticulously quantified the shifts in water storage and land subsidence resulting from the establishment of reservoirs, harnessing data on equivalent water thickness sourced from the GRACE mission. Meanwhile, Alshehri and Mohamed [38] conducted an in-depth analysis, utilizing GRACE to assess fluctuations in groundwater storage within Saudi Arabia, clearly highlighting the effectiveness of this method in investigating changes in groundwater resources.

The primary goal of this study is to assess the influence of the Hali dam construction on vegetation downstream in the arid Hali basin of Saudi Arabia. This research also examines the potential impact of local climate conditions within the basin, characterized by extreme heat, high evaporation, limited surface water, a prolonged dry season, and sporadic rainfall. To achieve these objectives, Landsat imagery time series are employed to track the changes in downstream vegetation after the dam's construction, while also considering the change in the equivalent water thickness (EWT) and the effects of climate variables, such as two meter surface temperature, total precipitation, total evaporation, and specific humidity. By leveraging satellite remote sensing data and model outputs, this research addresses the critical gap in our understanding of how the Hali dam affects vegetation, both before and after its construction. Additionally, it sheds light on the broader environmental consequences, including potential cropland expansion, associated with such infrastructure projects. This work contributes to a more comprehensive comprehension of their complex interactions.

2. Data and Method

2.1. Case Study

The Wadi Hali Basin is located within the Asir mountains and near the Red Sea coast [39], in the southwestern region of Saudi Arabia as shown in Figure 1. It is one of the largest basins in Saudi Arabia, located in the Southern Tihama Plain, with an average slope of 17.5 m km^{-1} and a total length of 160 km. The Wadi Hali Basin encounters sporadic rainfall, leading to flash floods crucial for aquifer recharge. Rapid runoff due to limited vegetation and extreme temperature variations affect its hydrology and water balance, making its study vital for resource management and environmental impact mitigation. The study area is in a hot desert climate based on [40], and this type of climate contains two types of seasons: long summers and short winters. Precipitation from the adjoining hills is collected within the watersheds and channeled toward the Red Sea [39]. The Hali basin has an average rainfall amount from 50 to 100 mm year^{-1}, and the headwaters (e.g., the initial source of a stream) of the Hali basin have an average rainfall amount from 300 to 600 mm/year [40]. The Hali Dam is in the Wadi Hali Basin on the Red Sea coast on the southwestern side of the Kingdom of Saudi Arabia, at Longitude of 41°30′00″E and Latitude of 18°44′00″N. The Red Sea coast of the Arabian Peninsula contains different ravines along the coast and has a limited amount of vegetation, except for a few sparse species of Prosopis Juliflora, halophytes, and mangroves (Avicennia marina). The Hali Dam is a gravity dam constructed in 2009 and has a catchment area of 5222 km^2 [39]. According to the Ministry of Environment, Water, and Agriculture in Saudi Arabia, several dam applications are flood control, irrigation, domestic water supply, and groundwater recharge. The dam has a total storage of 249,860,000 m^3 [39]. Its headwaters are located at an elevation of about 2000 m above mean sea level, extending west to the red sea.
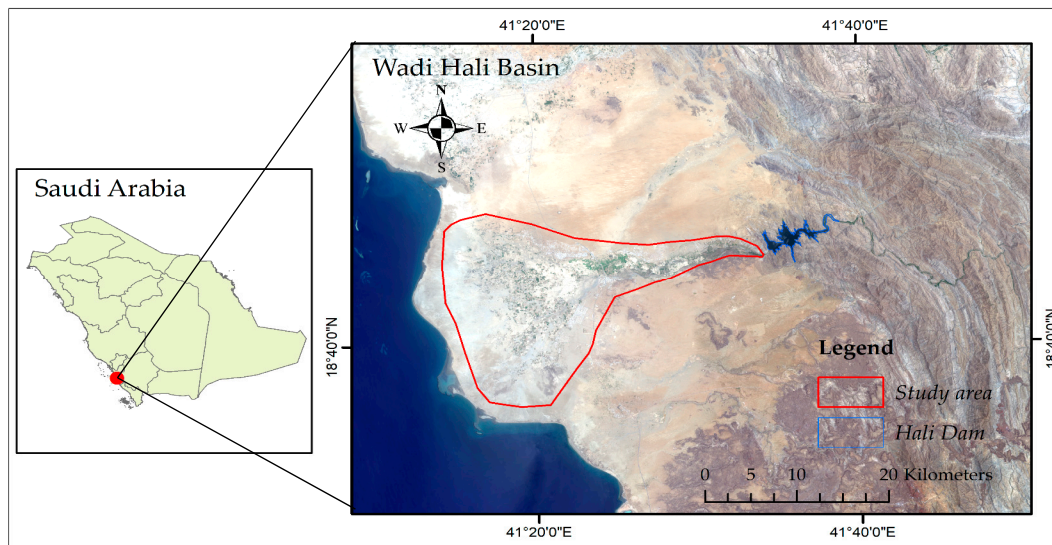
Figure 1. The geographical location of the study area.

2.2. Database

2.2.1. Satellite Data Source and Pre-Processing

The Landsat satellite images from various sensors, including Landsat-4 and 5, Landsat-7 ETM+, and Landsat-8, were obtained from the United States Geological Survey (USGS) (source: https://earthexplorer.usgs.gov, accessed on 22 October 2022). All images were acquired in levels and collections 1 and were carefully processed to ensure accuracy, involving radiometric and atmospheric corrections to enhance their quality. Cloudy and missing values in this study were processed using cloud masking and interpolation techniques. In this study, satellite images were selected based on three criteria: (1) cloud coverage of the satellite images must be less than 10 percent, (2) the availability of the image satellite series should be available over a long period to provide the ability to compare downstream changes before and after the dam construction, and (3) the data should be available over wet and dry seasons. Cloudy and missing values in the remote sensing images were processed using cloud masking and interpolation techniques. Satellite images were selected mainly for January and February for the wet season from 2000 to 2020. During the dry season from 2000 to 2020, satellite images were selected mainly for August and September. During these months, the most data were available in terms of availability, and these months were chosen because they represent the peak of each season. To achieve spatial and temporal resolution in the satellite imagery and meteorological data, multiple sensors and reanalyzed meteorological data were used in this study.

2.2.2. Climate Variables Selection and Data

Climatological data variables such as temperature, precipitation, humidity, evaporation, and wind speed are important parameters that describe a specific region's climate and its interaction with vegetation. In this study, temperature, precipitation, specific humidity, and evaporation were considered to investigate the impact of climate variables on vegetation areas' activities. This study considered climate data for the dry season from May to September and the wet season from October to February to investigate vegetation areas' response to climate variability. Climate data were acquired from the European Centre for Medium-Range Weather Forecasts Integrated Forecasting System, the fifth-generation reanalysis ERA-5 (source: https://cds.climate.copernicus.eu, accessed on 3 November 2022), and the Global Land Data Assimilation System (GLDAS) (source: https://giovanni.gsfc.nasa.gov, accessed on 14 November 2022), which have widely been used in previous studies [41]. This study used 21 years of climatic data, including two meter surface temperature, evaporation, and total precipitation from ERA-5 and specific

humidity from GLDAS for the period from 2000 to 2020 with a $0.1° \times 0.1°$ spatial resolution and monthly averaged time frequency.

2.2.3. Equivalent Water Thickness (EWT)

Gravity field variations due to Earth's mass changes were obtained from The Gravity Recovery and Climate Experiment (GRACE) mission [42]. Gravitational variations measured by GRACE are primarily due to water distribution on and beneath the Earth's surface over the terrestrial area [43]. Therefore, it can estimate the vertical changes in terrestrial water storage, including surface water, soil moisture, groundwater, canopy storage, and snow water equivalent [42]. This study used the monthly EWT product of JPL MASCON GRACE product Level-3 data (source: https://grace.jpl.nasa.gov, accessed on 18 November 2022) for the study area for the (available) period from April 2002 to December 2020.

2.3. Methods

Figure 2 summarizes the research method starting from collecting the data, including Landsat imageries and climate data from the ERA-5 and GLDAS models. The online acquisition of EWT data was conducted. All the imagery data were pre-processed, such as radiometric, geometric, and atmospheric corrections, which is a crucial step in preparing data before analysis. The NDVI calculation and supervised classification using Maximum Likelihood Classification (MLC) were applied to the satellite imagery before and after the dam construction. High spatial resolution Satellite pour l'Observation de la Terre images were used to evaluate the accuracy of the supervised classification. Change detection maps were produced before and after the dam construction (2000–2009 and 2010–2020, respectively). Afterwards, a Pearson correlation analysis and linear regression analysis were used to explore the relationship between the vegetation data acquired from the satellite imagery and both the climate and EWT data. In the following sections, all the steps taken to obtain the results presented in this study are explained in more detail.

2.3.1. Image Classification and Accuracy Assessment

Maximum Likelihood Classification (MLC) is one of the most commonly used parametric classifiers [44] to investigate different vegetation types' (e.g., natural vegetation and croplands) changes. In this method, pixels are classified based on their probability of belonging to a particular class. The covariance matrix is used to account for the variability of classes. For the MLC algorithm to perform correctly, it needs enough training sample plots with representative spectral signatures for each class. More details can be found in different textbooks, such as [45]. The Landsat images were classified using MLC, into natural vegetation, croplands, and bare areas. The classification of vegetation types involved data fusion, combining high-spatial-resolution imagery (SPOT) with the Landsat images. Additionally, supervised classification was performed using visual interpretation of the high-spatial-resolution images.

Performing an accuracy assessment is an essential step for the evaluation of classification results. As vegetation areas change, it is crucial to know the accuracy of the result before using it [46]. A confusion matrix, which is an array of numbers arranged in rows and columns that indicates how many sample units (pixels) are assigned to each category compared to what is actually in the ground, was used here. Moreover, is often used to derive descriptive and analytical statistics to determine classification accuracy. The high-spatial-resolution SPOT images acquired from King Abdulaziz City for Science and Technology of (1.5 to 10 m) for 2004, 2006, 2012, 2016, and 2021 were used to produce a stratified random sample for each vegetation class. Each image was used for an accuracy assessment evaluation for the corresponding years, assuming that no significant changes accrued within the seasons. Many samples were taken to attain high classification and accuracy results. Overall, 116 samples were considered for each year in each season to produce accurate assessment results.
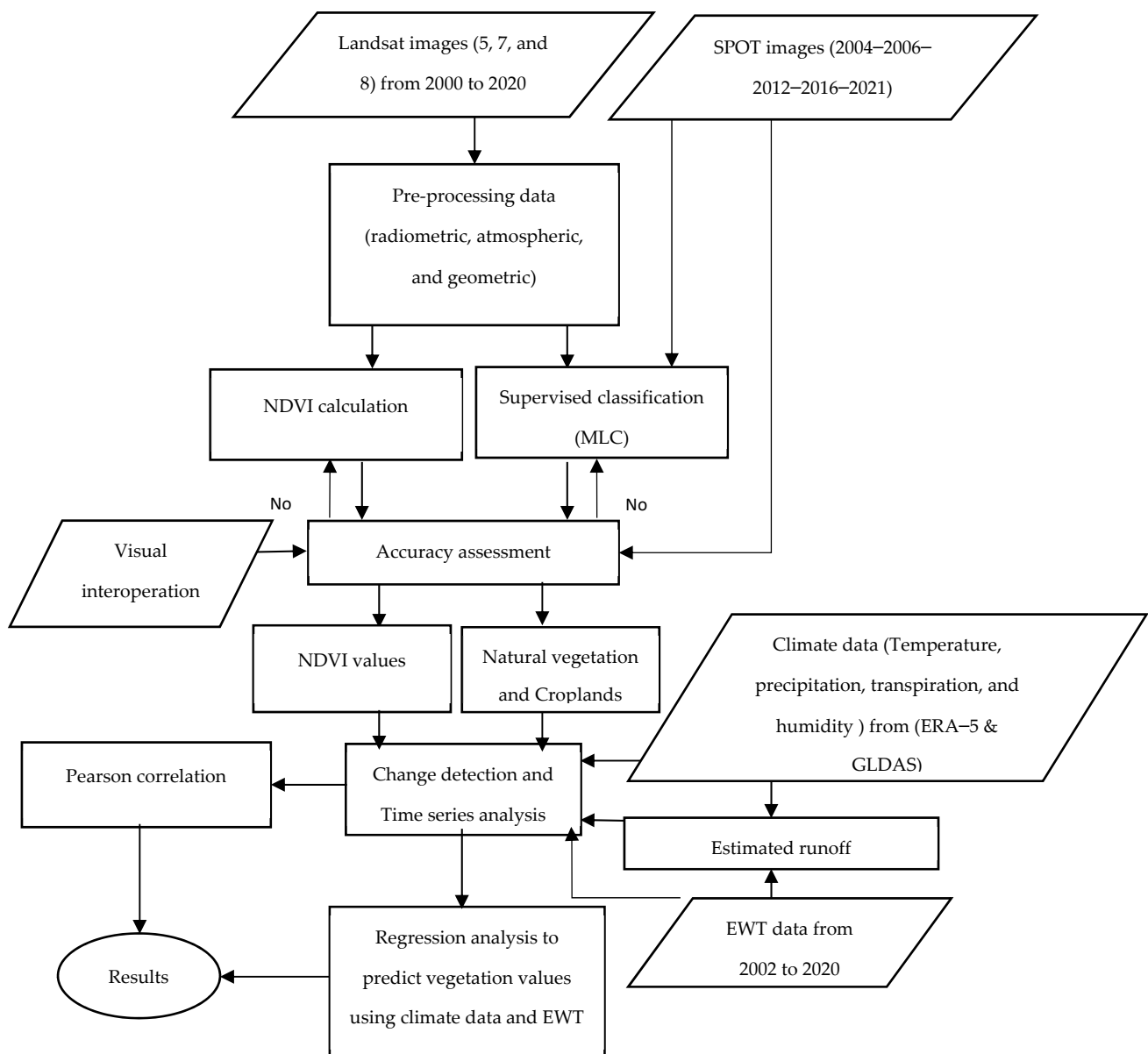
Figure 2. Flowchart of the applied methodology to analyze the vegetation changes in the Wadi Hali Basin before and after the Hali dam construction.

2.3.2. NDVI Calculation

The NDVI is an index that is widely used to describe vegetation variations. The NDVI is used to enhance the presence or absence of vegetation by generating the normalized band ratio. NDVI values range from +1 to −1, where positive values represent green cover while negative values indicate non-vegetative surfaces [31]. The higher the positive values, the more vegetation there is. A negative NDVI describes water bodies and built-up areas, while bare areas range from 0 to 0.03, and the values for healthy vegetation are typically between 0.4 and 0.76 for cropland and natural vegetation [47]. The NDVI index is calculated using the following equation:

$$NDVI = (NIR - RED)/(NIR + RED) \qquad (1)$$

In the case of Landsat-5 and 7, near-infrared (NIR) indicates band 4 and Red (RED) indicates band 3. Regarding Landsat-8, near-infrared (NIR) indicates band 5 and Red (RED) indicates band 4. The NDVI was calculated once for one month for each season (wet and

dry), resulting in two NDVI calculations for each year spanning from 2000 to 2020. The NDVI was calculated 9 years and 12 years before after dam construction, respectively. After the NDVI values were calculated for each season in every year, the mean NDVI was calculated before and after dam construction. The difference between the mean NDVI before ($NDVI_{mean\ before}$) and after ($NDVI_{mean\ after}$) the dam construction was calculated for each season. The results are presented as two maps illustrating each season's gain and loss of vegetated cover areas.

2.3.3. Estimation of Runoff

The terrestrial water budget encompasses various components, including precipitation (rain and snowfall), evapotranspiration (evaporation from soil and canopy, plant transpiration, and snow sublimation), runoff (surface and subsurface flow), and water storage within the land surface (such as snowpack, vegetation canopy, lakes, wetlands, and rivers) and subsurface (soil moisture and groundwater) [48,49]. The balance of precipitation (P), evapotranspiration (E), and runoff (R) is determined by the change in the water storage (S) at the Earth's surface. Due to the lack of ground data for stream runoff, Equation (2) was used to calculate the runoff for all the case studies:

$$R = P - E - \frac{\Delta S}{\Delta t} \tag{2}$$

where t represents time. All measurements are presented in millimeters. Additionally, the runoff, originally in cubic meters per second (m^3/s), is converted into millimeters by dividing it by the basin area. The time scale is monthly, and the data used are as mentioned in the data section.

2.3.4. Pearson's Correlation and Multivariate Regression Analysis

The Pearson's correlation coefficient evaluates the strength of the linear relationship between two variables by using the covariance matrix of the data and computing it. This study used Pearson's correlation coefficient to analyze the relationship between vegetation types (i.e., natural vegetation, croplands, and mean NDVI), climate variables (i.e., two meter surface temperature, precipitation, specific humidity, and evaporation), and EWT. This was to identify the major climate variables that impacted the vegetation areas of the study area from 2000 to 2020. The Pearson's correlation coefficient was applied to the time series for each season before and after the dam construction. This study used the *p*-value to test whether the calculated correlation between the variables was statistically significant.

The final step of this study was applying the multivariate regression analysis, which can determine the relationships between two or more variables, leading to a cause–effect understanding [50]. A multivariate regression analysis was applied to the NDVI using climate variables to evaluate if the variations in the EWT and climate variables' data could explain the NDVI variability before and after the dam construction. The first multivariate regression analysis was performed before the dam construction from 2002 to 2009, and the second one was applied after the dam construction from 2010 to 2020. The results are presented to assess the ability of EWT and climate variables' data to predict the NDVI variations over the two periods. The multivariate regression analysis model (Equation (3)) is estimated by,

$$y = \beta_0 + \beta_1 x_1 + \beta_2 x_2 + \beta_3 x_3 + \beta_4 x_4 + \beta_5 x_5 + e \tag{3}$$

In Equation (3), y represents the dependent variable (mean NDVI) and x represents the independent variables (EWT, two meter surface temperature, precipitation, evaporation, and specific humidity). β_0 is the intercept of y, and β_x is the changes in the mean of y or represents the slope of the regression line. *e* represents the model's equation error.

3. Results

3.1. Annual and Seasonal Variation of Vegetation Areas

3.1.1. Vegetation Areas Using Supervised Classification (MLC)

The vegetation areas' classification maps for the years from 2000 to 2020 for wet and dry seasons produced from the Landsat images are displayed in Figures 3 and 4, respectively. The figures illustrate the results for 5 years (2000, 2005, 2010, 2015, and 2020) and for the two seasons. The supervised classification shows natural vegetation and croplands. The vegetation areas of the study area changed considerably between 2000 and 2020 for both seasons. The average area covered by natural vegetation decreased by 25.5 percent from 2000 to 2020, while croplands increased by 48.4 percent from 2000 to 2020. Moreover, a comparison of the results before and after the dam construction shows that the average area covered by natural vegetation declined by 28.4 percent after the dam construction. In contrast, the croplands increased by 62.7 percent after the dam construction. This increase in croplands could have been due to various reasons, but irrigation plays a significant role, as it was one of the important reasons for the dam construction. This caused an increase in croplands and a decrease in natural vegetation areas due to the dam's impoundment of seasonal water flow after heavy rain, which used to support natural vegetation before the dam construction.
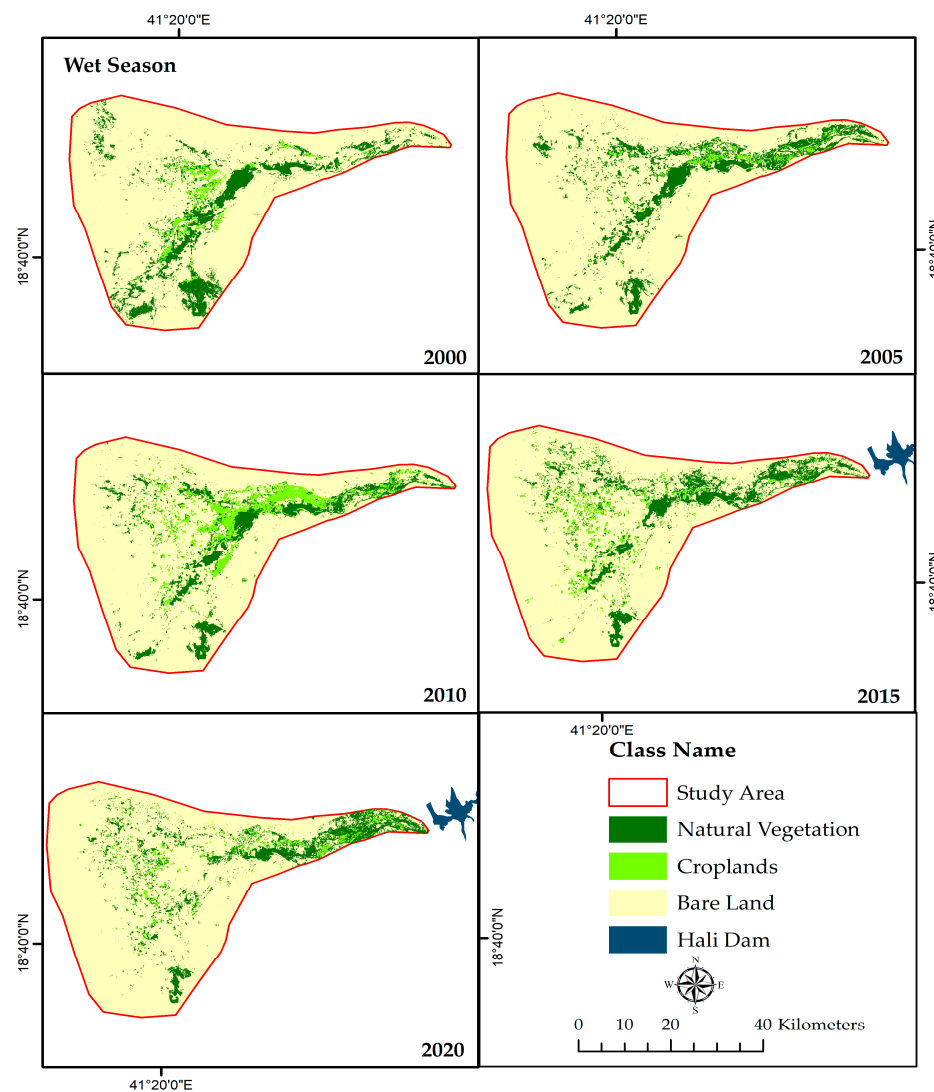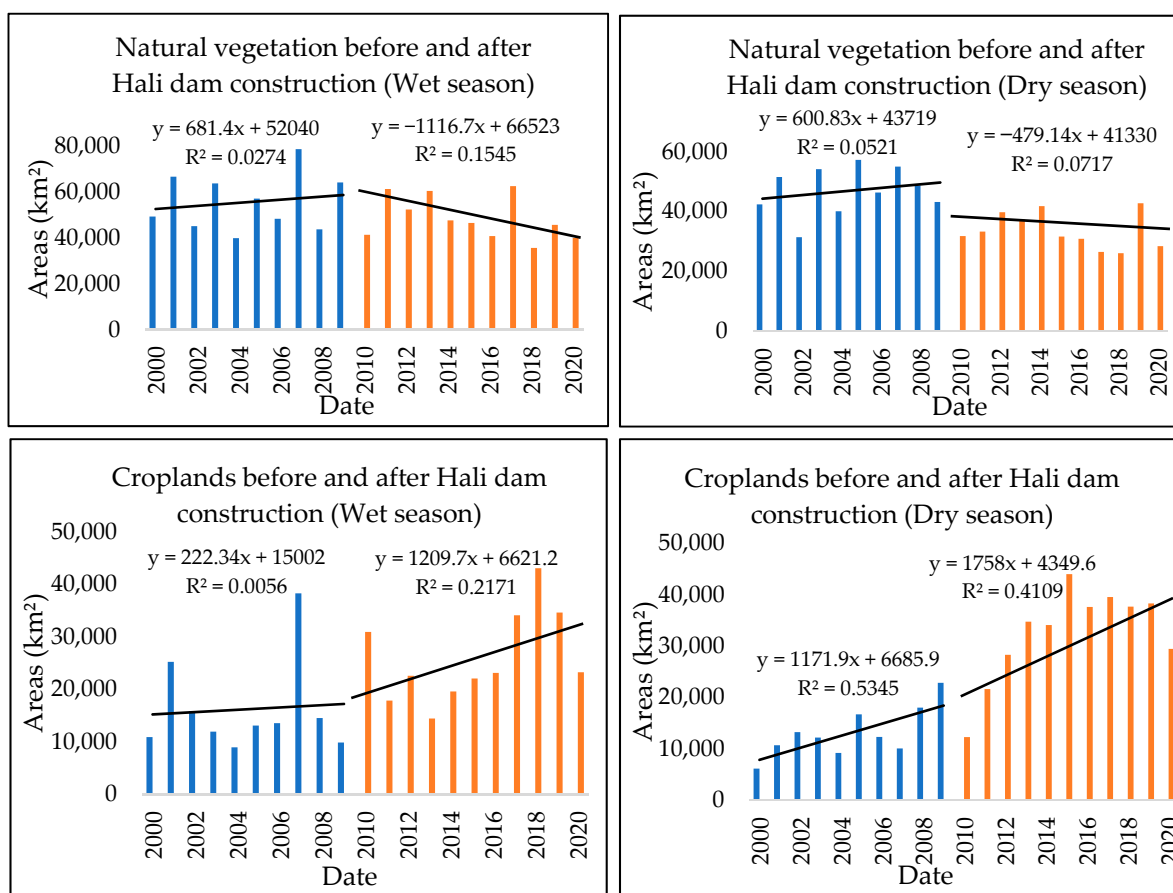

Figure 3. Supervised classification of the variation of the spatial distribution of vegetation areas for wet seasons for 2000, 2005, 2010, 2015, and 2020.
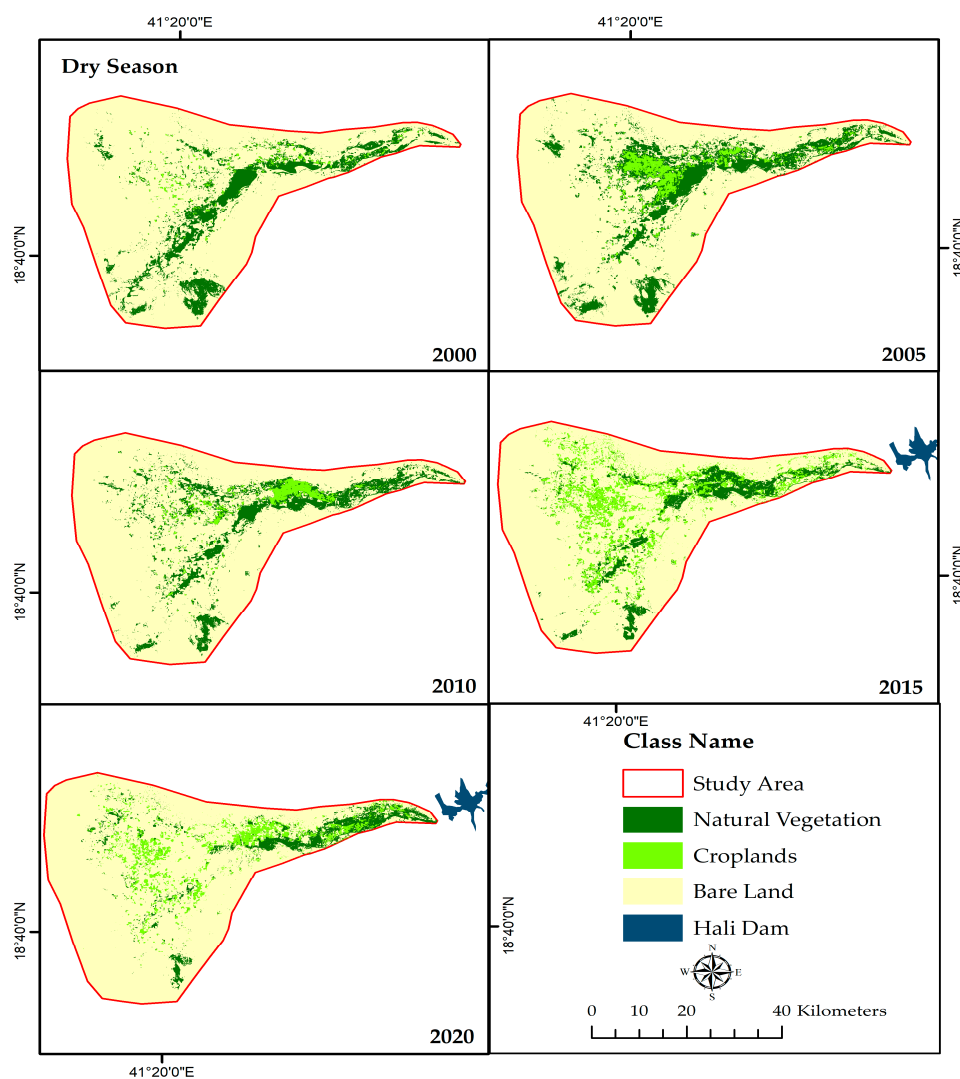
Figure 4. Supervised classification of the variation of the spatial distribution of vegetation areas for dry seasons for 2000, 2005, 2010, 2015, and 2020.

Figure 5 shows the bar chart of the total natural vegetation and cropland areas in km^2 over the study sites for the wet and dry seasons and for the period from 2000 to 2020. Before the dam construction (2009), the natural vegetation and croplands slightly increased in the two seasons. After the dam construction, the trend line decreased for natural vegetation and increased for the croplands in both seasons. Prior to the dam construction, there were increases of 681 km^2 and 600 km^2 in natural vegetation areas during the wet and dry seasons, respectively. Following the dam construction, natural vegetation areas experienced decreases of 1116 km^2 and 479 km^2 during the wet and dry seasons, respectively. On the other hand, before the dam construction, there were increases of 222 km^2 and 1171 km^2 in cropland areas during the wet and dry seasons, respectively. The significance of the trendlines for natural vegetation, both before and after the construction of the Hali dam, varied with the season. During the wet season, the *t*-test value was 2.306, with an associated *p*-value of 0.047. In contrast, during the dry season, the *t*-test value was −2.536, with a *p*-value of 0.032. Similarly, for croplands, the significance differed by season. During the wet season, the *t*-test value was 3.281, with a *p*-value of 0.010, while during the dry season, the *t*-test value was −8.188, and the *p*-value was 0.000. Following the dam construction, cropland areas experienced increases of 1209 km^2 and 1758 km^2 during the wet and dry seasons, respectively. The main crops grown in this region are sorghum, sesame, and millet [51]. These crops are warm season plants and their growth is usually from May to

October [52]. The cropland variation was significantly higher in the dry season compared to the wet season due timing of the growing season. The results suggested that the changes in the natural vegetation and croplands were associated with the dam construction. The decrease in the natural vegetation after the dam construction could have been due to the impoundment of the seasonal water flow by the dam construction. Moreover, the significant increase in the croplands after the dam construction could be associated with water management policies and dam applications, such as releasing water for agricultural irrigation from the dam.

Figure 5. The total areas of natural vegetation and croplands before and after the dam construction for wet and dry season.

3.1.2. Accuracy Assessment of Vegetation Areas Using Supervised Classification

As a result of the accuracy assessment of the image classifications, it was determined that the overall accuracy of the supervised classification was between 71 percent and 92 percent across all seasons. The accuracy assessment results were calculated using a confusion matrix and high spatial resolution of satellite imageries (SPOT) for 2004, 2006, 2012, 2016, and 2021 between image pixels to the actual feature in the ground, as shown in Table 1. As mentioned by Congalton [53], an accuracy assessment value greater than 70 percent is considered as acceptable to represent a perfect correspondence. In comparison, an accuracy assessment of less than 70 percent could indicate confusion between vegetation area types in the classification results. All the accuracy values in Table 1 are acceptable because they are higher than 70 percent. The average accuracy values were 76 percent for the wet season and 79 percent for the dry season. As a result, the final accuracy assessment for the classification was 77.5 percent. The highest accuracy was associated with the same years of the SPOT imagery that was used for the accuracy assessment classification, such as 2004, 2012, and 2016. However, the lowest accuracy values were

associated with the years that did not have the same years of SPOT imagery used for the accuracy assessment classification. Additionally, the lowest accuracy assessment in the 2010 wet season could be attributed to cloud contamination, which may significantly have impacted the classification accuracy.

Table 1. Supervised classification accuracy assessment results.

Year	Wet Season	Dry Season	Year	Wet Season	Dry Season
2000	81%	73%	2011	73%	80%
2001	73%	73%	2012	76%	92%
2002	72%	80%	2013	74%	82%
2003	75%	72%	2014	71%	80%
2004	79%	80%	2015	76%	81%
2005	78%	78%	2016	80%	82%
2006	76%	76%	2017	78%	78%
2007	78%	73%	2018	74%	80%
2008	75%	79%	2019	92%	87%
2009	74%	75%	2020	81%	87%
2010	71%	77%			

3.2. Annual and Seasonal Variation of NDVI

As explained in previous sections, the NDVI represents the greenness density and health of vegetation within each pixel of a satellite image. The NDVI of the study area changed considerably between 2000 and 2020 for both seasons. The wet season showed the highest NDVI values ranging between 0.34 and 0.74, with an average of 0.54, while, for the dry season, the NDVI ranged between 0.42 and 0.64, with an average of 0.53 between 2000 and 2009. However, after the dam construction, in the wet season, the highest NDVI values ranged between 0.39 and 0.69, with an average of 0.54, while, for the dry season, they ranged from 0.28 to 0.41, with an average of 0.34. This indicates a 26 percent decline in the average NDVI for the dry season over the study area. Overall, the comparative analysis before and after the dam construction showed higher NDVI values both in terms of magnitude and spatial distribution before the dam construction.

NDVI variations were further analyzed to provide a clear understanding of how they varied over time. Spatially averaged NDVI time series from 2000 to 2020 for the wet and dry seasons were calculated from the Landsat images and are displayed in Figure 6a,b. The mean NDVI for the wet and dry seasons before the dam construction were 0.115 and 0.102, respectively. Moreover, the mean NDVI for the wet and dry seasons after dam construction were 0.103 and 0.089, respectively. There was a variation in the annual mean NDVI before the dam construction. Before the dam construction, there were increases of 0.0007 and 0.0019 in the NDVI values during the wet and dry seasons, respectively. Following the dam construction, the NDVI values experienced decreases of 0.0027 and 0.0028 during the wet and dry seasons, respectively. The significance of the trendlines for the mean NDVI, both before and after the construction of the Hali dam, varied with the season. During the wet season, the *t*-test value was 2.591, with an associated *p*-value of 0.046. In contrast, during the dry season, the *t*-test value was 1.452, with a *p*-value of 0.180. A distinct decline in the mean NDVI values can be observed after the dam construction, starting in 2011 and 2012 for both seasons. This trend could be attributed to the impoundment of water flow caused by the dam construction. An increase in the NDVI values after the dam's construction in 2011 could be associated with the expansion of croplands. Before the dam construction, the trend in mean NDVI values slightly increased, which could have been due to the amount of precipitation and a larger amount of surface runoff. A noticeable decrease, however, can be seen after the dam construction, especially during the dry season. This could have been due to the restriction of water downstream of the dam, which may have resulted in a reduction in regeneration and vegetation greenness.
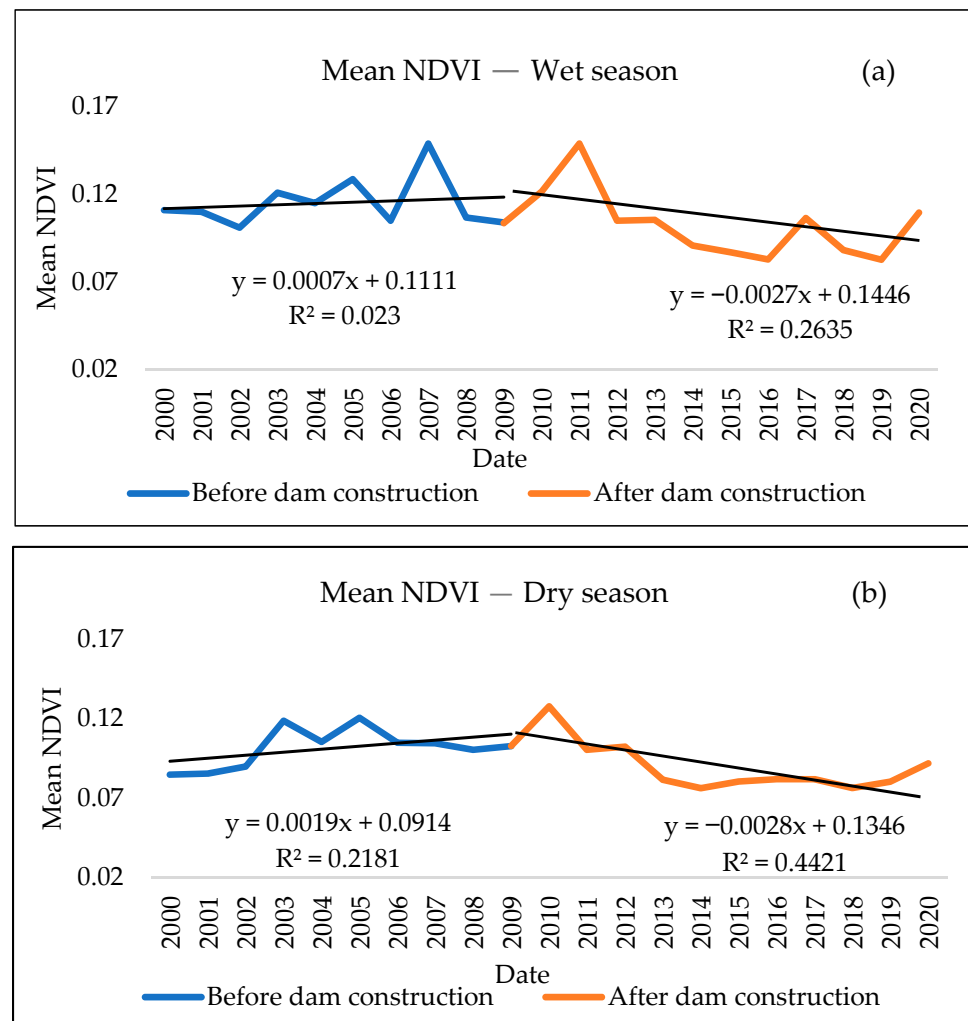
Figure 6. The mean NDVI trendlines for wet season (**a**) and dry season (**b**) variation from 2000 to 2020.

3.3. Spatial Variations of NDVI

Figure 7 represents the spatial variations in the gain and loss of downstream vegetation areas using the NDVI values. The red color in Figure 7 represents the loss of vegetation areas downstream of the dam and coincides with the natural vegetation. The green color in this figure represents gains in vegetation areas downstream of the dam, which correspond to the croplands. The significant vegetation changes before and after the dam construction for the two seasons are in areas far from the dam, such as in the middle of the stream and the alluvial fan areas. The alluvial fan areas are deposits of gravel, sand, and even smaller sediment particles, such as silt [54]. These areas are relatively more fertile than other soil types. Therefore, the dam impounded this sediment to be transported by seasonal water flow from the Hail basin catchment to the downstream alluvial fan areas [55], potentially impacting the vegetation areas downstream. The negative impact represented in red color, which mainly represents the natural vegetation area, could be due to several reasons; for example, downstream wetland areas could decrease due to the dam impoundment of water to support downstream vegetation areas. The gained areas mostly show the croplands, possibly due to the dam's irrigation water.
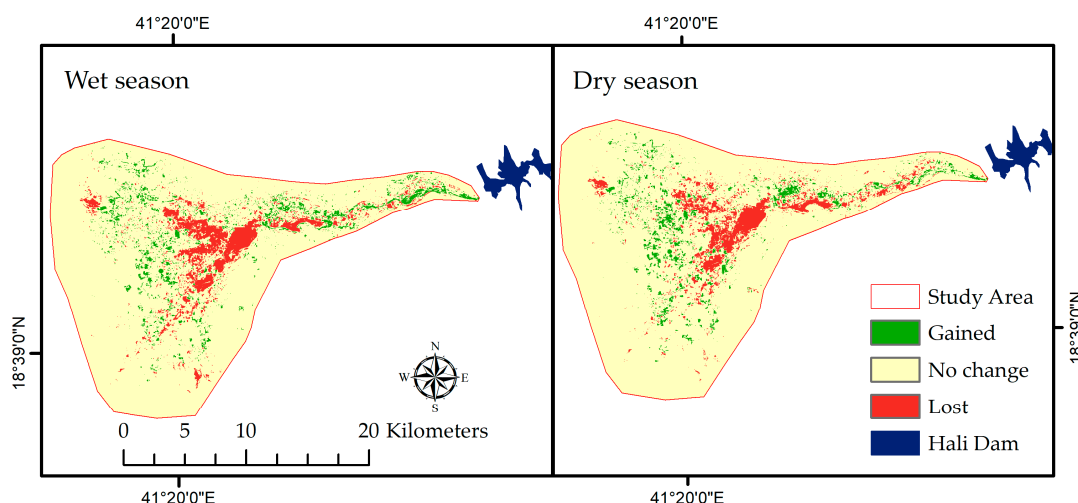
Figure 7. The spatial distribution of the differences in NDVI before and after the dam construction for wet and dry seasons.

3.4. Inter-Annual Variations of Climatic Variables

To better investigate the vegetation trends and the potential impact of climate variabilities, this study used monthly climate model data from 2000 to 2020. Figure 8a shows the monthly two meter surface temperature changes in the study area. No significant change in the average two meter surface temperature, before the dam construction (30.23 °C) and after the dam construction (30.25 °C), was found. While some increase in the amount of total precipitation can be seen (e.g., in 2001 and 2004), the overall trend of precipitation was slightly negative from 2000 to 2015, which could, in turn, impact the mean NDVI and the vegetation areas variations. Moreover, EWT could contribute to the change in the variation in the NDVI, as will be discussed in Section 3.5. Almazroui et al. [56] reported a similar decline for the Saudi Arabia's precipitation from 1994 to 2009. Moreover, Hasanean and Almazroui [40] reported high precipitation accrued in 2001 and 2004 in the wet season. In 2016 and 2017, there was a high amount of precipitation in the study area. This could have been due to the presence of temperature anomalies in this period [57]. The mean total monthly precipitation before and after the dam construction was relatively close: 3.05 mm and 2.88 mm, respectively. Despite slight changes in the precipitation and the two meter surface temperature before and after the dam construction, these results showed no clear evidence of climate variability in the area that could have been responsible for the considerable observed vegetation decline after 2009.

Figure 8c shows the monthly specific humidity, which refers to the quantity of water vapor contained in a unit quantity of air, expressed as kilograms of water vapor per kilogram of air. The average monthly specific humidity before the dam construction was 0.015 kg kg^{-1} and 0.016 kg kg^{-1} after the dam was constructed. Therefore, this increase is insignificant. as it shows no overall considerable change in evaporation and specific humidity before and after the dam construction. This suggests that vegetation changes could be primarily related to the water (surface and subsurface) changes that could be impacted by the dam construction. Figure 8d shows the monthly total evaporation from 2000 to 2020, with negative values indicating evaporation and positive values indicating condensation. The total evaporation displayed higher values in some years, such as 2016 and 2017. The increase in evaporation can be explained by the increasing the temperature values and the higher precipitation values in 2016, and 2017. Previous research findings have indicated a roughly 50% increase in evaporation from 2011 [30]. Overall, the variations in total evaporation were similar to the changes in total precipitation. Nevertheless, the mean total monthly evaporation before the dam construction (−0.00031 m water equivalent) was slightly higher than that after the construction of the dam (−0.00029 m water equivalent).
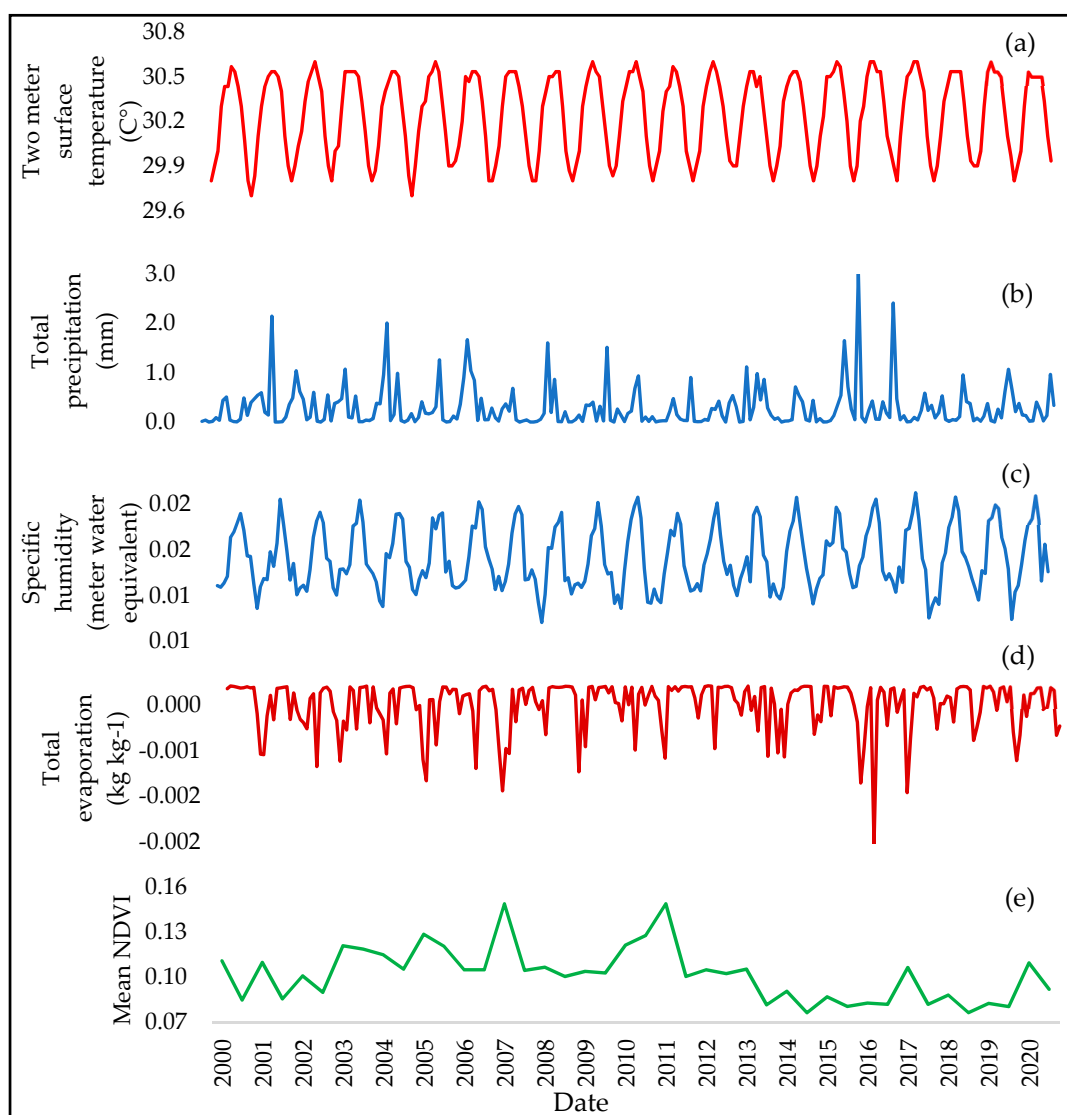
Figure 8. Two meter surface temperature (**a**) and total precipitation (**b**) from 2000 to 2020 ERA-5. Monthly specific humidity kg kg^{-1} from 2000 to 2020 GLDAS (**c**) total evaporation in meter water equivalent from 2000 to 2020 ERA-5 (**d**) and with mean NDVI (**e**).

3.5. Annual Variations of EWT

Figure 9 represents the monthly EWT in the land, with a clear negative trend from 2005 to 2020. Except for some seasonal variations and strong anomalies (e.g., in 2017), the EWT overall changes and trends, particularly after 2009, were different than the climate variables' changes, such as precipitation and evaporation. The EWT and mean NDVI increased between 2002 and 2007, while precipitation decreased. A similar relationship was observed in several other studies, such as during periods of no precipitation, where soil water content increased and was attributed to a variety of environmental and climatic factors [58,59]. A clear reduction in both EWT and the mean NDVI exists after 2003 and 2011, respectively. The reduction in the EWT could have been due to agriculture's continuous depletion of groundwater over the past years [60]. As demonstrated by Alshehri and Mohamed [38], the agricultural sector predominantly contributes to the significant upsurge in groundwater extraction on the northern side of Saudi Arabia, and a similar scenario can be observed in the southern regions as well. In addition, the Wadi Hali Basin's arid climate results in a limited natural recharge of groundwater. Low and irregular precipitation, coupled with high evaporation rates, hinder the replenishment of groundwater aquifers [61]. It is expected that the EWT and NDVI time series share similar variations, since there is

a close relationship between soil moisture variations and vegetation changes. Overall, changes in EWT were negatively impacted by decreasing rainfall, dam construction, and high depletion by anthropogenic activities of groundwater, which consequently affected the vegetation changes and water stored in the land.
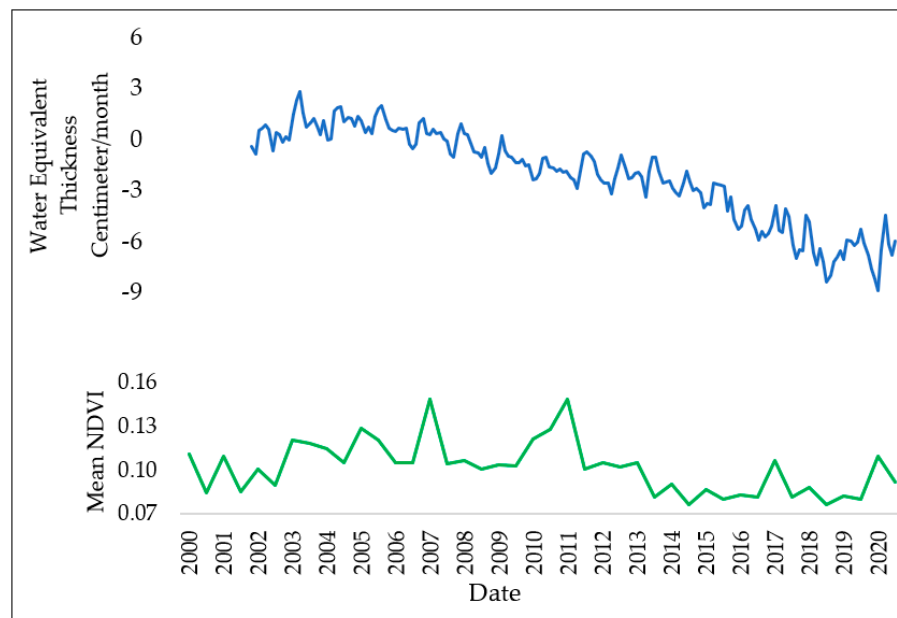
Figure 9. Equivalent Water Thickness (EWT) centimeters/month from 2002 to 2020 GRACE with mean NDVI.

3.6. Monthly Variations of Runoff

The provided calculations illustrate the monthly changes in downstream runoff both before and after the dam's construction. In Figure 10, the period before the dam's construction demonstrates a considerable range of runoff variability. Certain months, like December, exhibit minimal runoff with values close to zero, implying limited water flow due to low precipitation. Conversely, months like April show a higher runoff, reaching 106.2 mm, indicating elevated water flow potentially due to precipitation; Almazroui [62] indicated that the highest average rainfall that occurred was in April, with positive changes from 1981 to 2010. These fluctuations underscore the inherent monthly runoff variability before the dam's establishment. Following the dam's construction, the monthly runoff data continue to exhibit variability due to the inadequate provision of the flow downstream. Some months witnessed heightened runoff, such as 97.5 mm, indicating periods of increased water flow. After 2007, the estimated runoff experienced a decline, followed by an increase after 2010, which could be associated with a rise in NDVI values in 2011, and subsequently, another decline in 2012. This trend closely parallels the observed fluctuations in the NDVI values. The post-2015 period witnessed increased water flow due to the dam reservoir's elevation. As the dam reservoir capacity increased, the necessity to release water led to heightened water flow, as evidenced post-2015. The presence of the dam significantly influenced runoff patterns during this period, potentially resulting in modified flow dynamics compared to the pre-construction phase. The observed changes in estimated stream runoff may provide insight into alterations in NDVI values. This alignment between runoff patterns and NDVI changes suggests an interconnected relationship between water flow dynamics and vegetation health. Overall, the estimated runoff results can explain some of the changes in the NDVI variations and highlight shifts in the flow regulation by the dam, as these results are influenced by human activities, climate factors, and changes in water storage [63].
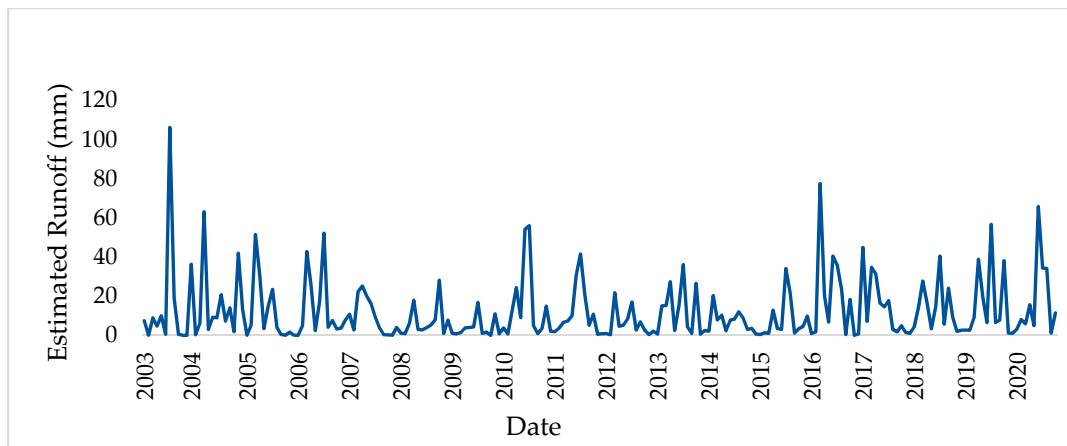
Figure 10. Monthly changes in runoff, which is the flow of water in streams, both before and after dam construction.

3.7. Correlation Coefficient Analysis

Climate variables and soil water availability are the main driving forces for vegetation [64]. In this section, the Pearson correlation values between the NDVI, natural vegetation, croplands, climatic variables (i.e., precipitation, evaporation, temperature, and humidity), and EWT are presented in Table 2, showing a strong positive correlation ranging from 0.66 to 0.80, with a significant $p < 0.05$ between vegetation types and NDVI with precipitation for the wet season before the dam construction. Moreover, there was a moderate to strong positive correlation ($p < 0.05$ for only natural vegetation) between vegetation types and NDVI with two meter surface temperature in the dry season before dam construction.

Table 2. Pearson correlation and *p*-value of vegetation type and NDVI with climate variables and EWT.

	Precipitation		Evaporation		Temperature		Humidity		EWT	
	R	P	R	P	R	P	R	P	R	P
Before Dam Construction: Wet Season										
Natural vegetation area	**0.77**	0.009	**−0.77**	0.009	−0.36	0.312	−0.05	0.989	0.1	0.82
Croplands area	**0.66**	0.039	**−0.58**	0.082	−0.33	0.353	−0.08	0.822	−0.3	0.467
Mean NDVI	**0.8**	0.005	**−0.76**	0.011	−0.14	0.708	0.42	0.232	0.24	0.566
After Dam Construction: Wet Season										
Natural vegetation area	0.04	0.899	0.41	0.207	0.03	0.941	**−0.52**	0.103	**0.57**	0.065
Croplands area	0.04	0.916	0.29	0.382	0.22	0.516	**0.62**	0.04	**−0.66**	0.023
Mean NDVI	0.03	0.927	0.2	0.557	−0.13	0.697	−0.17	0.612	**0.5**	0.157
Before Dam Construction: Dry Season										
Natural vegetation area	0.28	0.43	0.45	0.188	**0.72**	0.019	0.25	0.477	0.34	0.125
Croplands area	−0.25	0.487	0.23	0.524	**0.54**	0.33	−0.56	0.092	−0.5	0.204
Mean NDVI	−0.07	0.851	−0.1	0.775	**0.56**	0.09	0.13	0.704	0.11	0.79

Table 2. *Cont.*

	After Dam Construction: Dry Season									
	Precipitation		Evaporation		Temperature		Humidity		EWT	
	R	P	R	P	R	P	R	P	R	P
Natural vegetation area	0.12	0.715	−0.1	0.762	−0.28	0.4	0.29	0.376	0.48	0.276
Croplands area	0.11	0.74	−0.05	0.893	0.42	0.199	0.38	0.245	−0.49	0.155
Mean NDVI	−0.17	0.626	0.27	0.428	−0.18	0.595	−0.28	0.395	0.5	0.143

The evaporation correlation with vegetation areas and NDVI, as shown in Table 2, mainly followed the precipitation correlation values. For example, in the wet season, as the precipitation correlation became strongly positive, the evaporation became strongly negative with vegetation areas and NDVI. Regarding the specific humidity, the correlation between vegetation areas and humidity was ambiguous due to the climate characteristics in arid areas. After the dam construction, for both seasons, the Pearson correlation between vegetation changes and climate variables was mostly very low. Nevertheless, strong correlations can be seen between EWT and both vegetation types and NDVI after the dam construction. These Pearson correlation values agree with the previously presented results, where NDVI variations followed climate variables patterns before 2009. However, lower Pearson correlations can be seen after the dam construction, especially during the dry seasons. The pattern of NDVI variations is different and better match those of EWT. This can be explained by the impact of the dam on the downstream soil moisture and groundwater changes, as well as groundwater withdrawal for agriculture, which are better reflected in the EWT data. The difference in the Pearson correlations before and after dam construction could also be due to the impoundment of water flow by the dam construction.

3.8. Multivariate Regression Analysis

Multivariant linear regression was used to assess the variations in EWT and climate variables on NDVI variations before (2000–2009) and after (2010–2020) the dam construction. This was performed for two different scenarios: (1) modeling the NDVI only based on climate variables (i.e., precipitation, two meter surface temperature, evaporation, and specific humidity without EWT) and (2) modeling the NDVI using all the variables, including EWT. This was performed to examine the impact of EWT on the NDVI changes that were found to be considerable in previous sections. In the multivariant linear regression model, the NDVI was considered to be a dependent variable, while EWT and climate variables were independent variables that drove the variation in NDVI.

Figure 11A,B show the results of the multivariant linear regression applied to assess the variations in the NDVI using only climate variables before (Figure 11A) and after (Figure 11B) the dam construction. The R^2 value was found to be 0.76 before the dam construction from 2002 to 2009 between the observed and modelled NDVI. It indicates that 76 percent of the variations in the NDVI before the dam construction were driven by climate variables. On the other hand, the Pearson correlation between the observed and modeled NDVI after the dam construction was very weak. The R^2 value was 0.22 after the dam construction from 2010 to 2020. Therefore, using only climate variables to model the variation in the NDVI was mainly useful before the dam construction but not after. EWT data may be essential for modelling the variation in the NDVI that suggests the important role of groundwater and soil moisture.

Figure 12 demonstrates the results of the second scenario, where all the variables, including EWT, were used to predict the NDVI variations. As in Figure 12A, the Pearson correlation between the observed and predicted mean NDVI before the dam construction was strong in the case study. The R^2 value was 0.85 before the dam construction from 2002 to 2009. It indicates that 85 percent of the variations in the NDVI before the dam construction were driven by climate variables and EWT. This, which was higher than the first scenario where only climate variables were assumed, clearly shows an impact of the water stored in

the land on the vegetation. After the dam construction, the correlation between the observed and modeled NDVI after the dam construction was weak (Figure 12B). Nevertheless, the R^2 value (0.42) was higher than the first scenario after the dam construction from 2010 to 2020. It indicates that, while adding EWT to the variables increases the correlation between the modelled and observed NDVI, a considerable discrepancy between the NDVI variations and other variables exists. Overall, the NDVI variations did not follow the climatic pattern as they did before the dam construction. The changes in the correlation before and after the dam construction could have been due to changes in the downstream ecosystem. The dam construction impoundment of the seasonal water flow may have contributed to a decrease in the R^2 to 0.42.
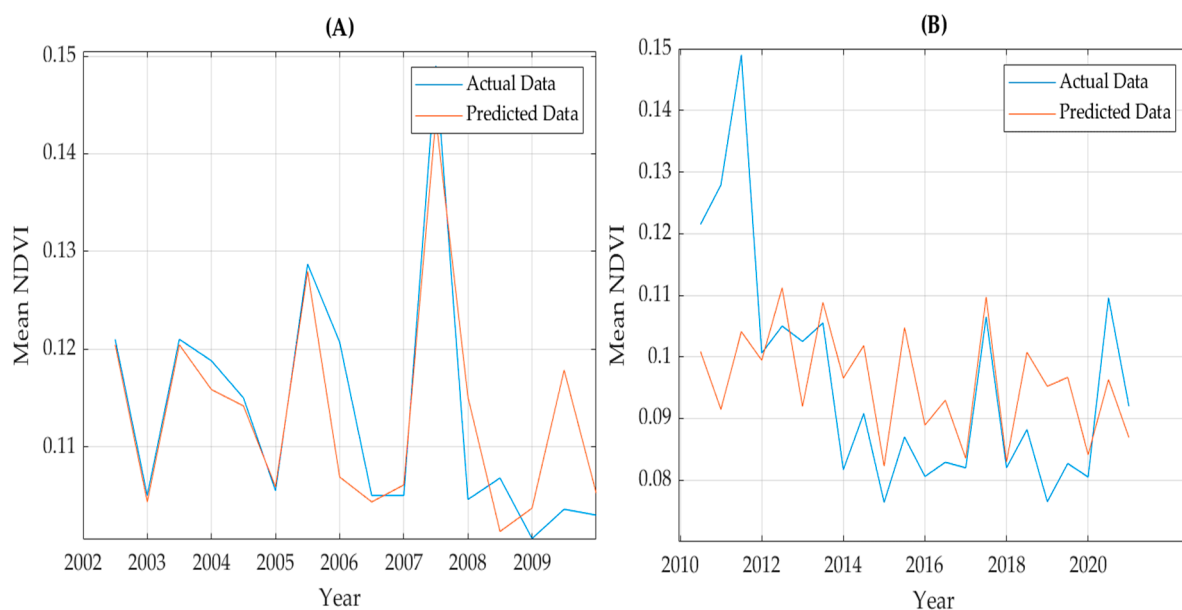
Figure 11. Modelling the mean NDVI variations using only climate variables' data including 2 m surface temperature, total precipitation, total evaporation, and specific humidity before the dam construction 2002 to 2009 as number (**A**) and after the dam construction 2010 to 2020 as number (**B**).
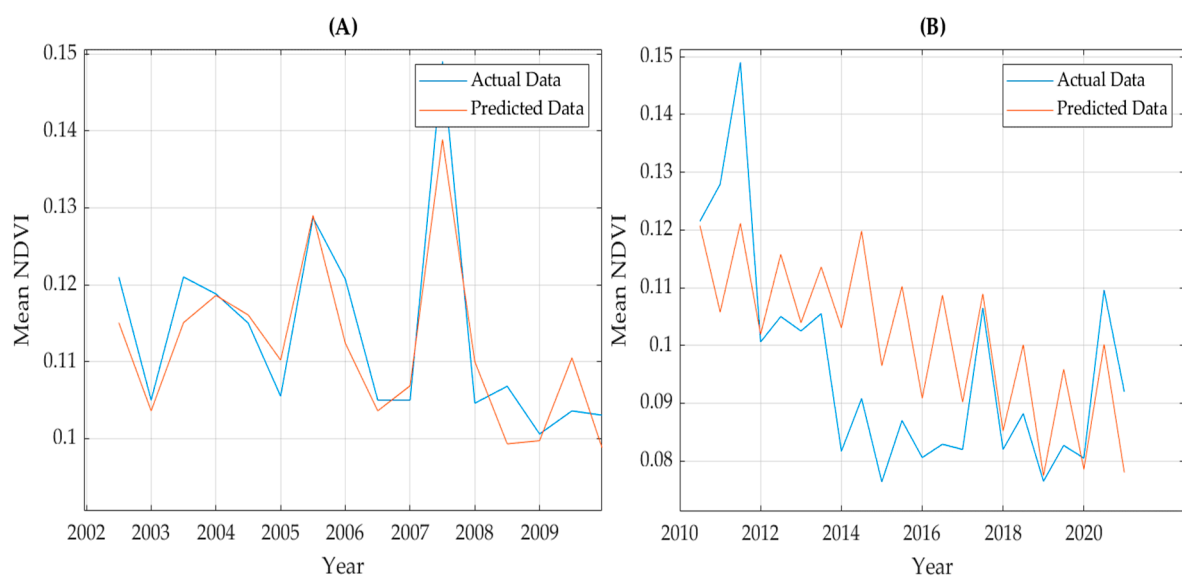
Figure 12. Modelling the mean NDVI variations using EWT and climate variables' data including 2 m surface temperature, total precipitation, total evaporation, and specific humidity before the dam construction 2002 to 2009 as number (**A**) and after the dam construction 2010 to 2020 as number (**B**).

4. Discussion

Based on Figures 3–5, croplands have been increasing since 2009 as one of the important purposes of the dam. The results suggest that human activities and croplands influenced by the dam have been extended at the expense of natural vegetation. Such activities, however, should be studied in more detail in studies. The NDVI time series and trends, as shown in Figure 6, showed a decreasing trend for both the wet and dry seasons after the dam construction. Moreover, the inter-annual vegetation NDVI and natural vegetation declined significantly after the dam construction. A considerable difference was found in the correlation between natural vegetation, croplands, and mean NDVI with climate variables before and after the dam construction, which could be explained by the impact of the dam on the region's environment. Prior to the dam construction, the NDVI and vegetation types in the study area were highly correlated with the surface temperatures and total precipitation for both seasons. These results agree with the relevant literature. For example, Xie et al. [20] and Tong et al. [23] suggested a strong positive correlation between vegetation and climate variables, especially for precipitation and temperature, which is similar to our findings before the dam construction. However, after the dam construction, the correlation between vegetation and climate variables was much lower, especially for the total precipitation, which is a critical climate variable for vegetation area. Such a correlation decrease could have been due to the dam's impacts. For example, stopping seasonal water flow to the study area could influence the vegetation growth and distribution in the study area. In addition, the presence of the dam influenced runoff patterns during this period, potentially resulting in altered flow dynamics compared to the pre-construction period. The change in the estimated stream runoff could be indicative of the alteration in the NDVI values. Therefore, the dynamic relationship between runoff patterns and vegetation health underscores the impact of the dam on flow dynamics and vegetation changes, influenced by human activities, climate factors, and alterations in water storage.

Before the dam construction, precipitation and particularly seasonal runoff water from the eastern mountains were the primary sources of vegetation area and soil moisture. Disrupting the runoff via the application of the Hali Dam was found to significantly affect vegetation growth and greenness. For instance, before the construction of the dam, water flowing from upstream to downstream transported sediments, which often contained significant nutrient content. Hence, the post-dam scenario of reduced water flow due to the reservoir might account for the diminished soil nutrient availability [65]. This decrease in water volume led to a decreased transport of sediments downstream, subsequently contributing to the scarcity of nutrients in the soil [66]. The decline in the presence of fine particles and nutrients within the soil could potentially yield detrimental repercussions for vegetation located downstream, including adverse impacts on the growth and vitality of plants and trees. Moreover, high temperatures and rapid evaporation can limit the water absorption from the precipitation by the soil in the areas. Furthermore, temperature increases of 1 °C and 5 °C could potentially lead to reductions in surface runoff of 115–184 Million Cubic Meter (MCM) and 600–960 MCM per year, respectively [67,68]. In a study conducted by Tarawneh and Chowdhury [30], an evaluation of temperature and rainfall trends across various regions in Saudi Arabia was undertaken. The outcomes revealed that both linear and Mann–Kendall analyses demonstrated a rise in temperature across all regions and a reduction in rainfall in multiple areas. These changes notably affect vegetation areas. Research conducted by Mallick et al. [69] suggested that rainfall emerges as the primary determinant in shaping the distribution of vegetation within these regions. As Saudi Arabia experiences rising temperatures and altered rainfall patterns, the resulting changes in climate dynamics are proving to be one of the major factors that shape the distribution and health of vegetation across the study area. Therefore, the decrease in natural vegetation during the dry season may indeed be related to the construction of dams. Dams can impact seasonal water flow, potentially leading to a reduced water availability for vegetation, especially during the dry season. It is possible that the decrease in vegetation coverage during the dry season is also related to the impact of drought. Drought conditions

can independently affect vegetation health by reducing water availability, and this impact may be exacerbated by dam construction.

The slight changes in the climate variables, as shown in Figure 8, may have led to slight changes in the vegetation area. However, more significant changes in human activities, e.g., through the dam construction, can cause similar changes in the total vegetation area. Despite slight changes in the precipitation and two meter surface temperature before and after the dam construction, these results showed no clear evidence of the climate variability impacts on the area and, correspondingly, the vegetation decline after 2009. The relationship between climate and vegetation dynamics can be complex, influenced by various factors, including hydrological changes due to dam construction, land use alterations, and ecological processes. Therefore, while the presented meteorological data may not reveal an explicit link between climate variability and vegetation decline, a comprehensive assessment of multiple factors is essential to unravelling the intricate web of influences on the ecosystem. Regarding the cropland expansion and decrease in the EWT, there are several papers that have examined the relationship between groundwater use and cropland expansion in Saudi Arabia. A comprehensive study was conducted by the International Water Management Institute (IWMI) [70]. The study found that groundwater use has been a major driver of cropland expansion in Saudi Arabia since the 1970s. The study also found that the expansion of cropland has led to a decline in the groundwater in many parts of the country. Another study by Alshehri and Mohamed [38] indicates that the agriculture sector is largely responsible for the dramatic increase in groundwater extraction in Tabuk areas, which clearly shows a decline in the EWT.

This study was able to identify a noticeable link between the NDVI and both climate variables and EWT variations. According to Figure 11A, using only climate variables, one could model the NDVI variation to a high degree before the dam construction. This modeling can be performed more successfully with a combination of climate variables and EWT before the dam construction (cf. Figure 12A). However, Figure 11B suggests that climate variables only were not able to accurately model the variation in the mean NDVI after the dam construction. Adding the EWT data, however, can improve the modeling skill to some extent (Figure 12B). Including EWT as the influencing factor in the multivariate regression analysis led to improved results with a higher R^2 value, which is important in estimating and representing the roles of groundwater and soil moisture [71]. According to the literature, EWT can be used to represent the impact of human variables on the total vegetation area [63,72,73]. In Pan et al. [72], human-induced evapotranspiration was detected in the Haihe River basin of China using EWT. Based on their findings, GRACE has the capability to detect anthropogenic signals over regions with a high groundwater consumption. The use of underground water for irrigation, water flow prevention by dam construction, and decreased soil moisture can lead to a negative trend in the EWT time series. Correspondingly, this can impact the total vegetation area directly by limiting soil moisture and increasing sand movement and soil salinity. EWT contributes to increased vegetation greenness, independent of climate variables. In addition, this exerts supplementary stress on the system, thereby jeopardizing both the sustainability of vegetation and the robustness and yield of crop production within this region. Furthermore, projections of future climate change, extrapolated from temperature and precipitation data, could potentially contribute to a decrease in the replenishment of groundwater resources. The research has limitations in fully analyzing hydrological components due to data constraints, including average daily and monthly flows and environmental flow. Future research should explore additional factors like Land Use Land Cover (LULC), soil components, hydrological components, wetlands, and groundwater's impact on downstream vegetation. Moreover, integrating high-spatial-resolution satellite imagery or a combination of high and medium spatial resolution can enhance accuracy assessments for smaller study areas.

5. Conclusions

Based on the characteristics of the selected study area, dam, and related reservoirs, and using 21-year (i.e., 2000–2020) meteorological and remote sensing data, this study aimed to detect changes in the vegetation areas downstream of the Hali Dam in the Wadi Hali Basin. Notably, the change in the estimated stream runoff could represent the change in the NDVI values. The NDVI results revealed a considerable decline after the dam construction in the dry season. This was primarily associated with blocking the seasonal runoff water by the dam and increasing cropland areas due to dam irrigation. There was no significant change in the climate variables before and after the dam construction, which may indicate weak impacts of climate variability on the area and, correspondingly, the vegetation decline after 2009. A significantly stronger correlation between vegetation changes and precipitation and temperature variations was observed before the dam construction. According to the multivariate regression analysis, 85 percent of the variations in the mean NDVI were driven by climate variables and EWT. On the other hand, it was found that only 42 percent of the variations in the NDVI were driven by climate variables and EWT from 2010 to 2020 for both the dry and wet seasons. Another analysis with the multivariate regression analysis using only the climate variables to model the NDVI variations showed that, before the dam construction, climate variables may have caused the variation in the NDVI values (with an R^2 of 0.76), but not after the dam construction (with an R^2 of 0.22). Despite these marginal shifts in climate and EWT variable metrics, the interplay of factors driving the substantial vegetation decline remains intricate and multifaceted. While these metrics provide valuable context, they alone might not unveil the complete picture of climate variability's impact on the area. Other factors that impact downstream vegetation areas, such as Land Use Land Cover (LULC), soil components, and wetlands, are important to be considered in future research. In addition, the hydrological components were not fully analyzed and incorporated into the research due to limitations in obtaining these data, such as average daily and monthly flows and environmental flow. Using high-spatial-resolution satellite imagery or combining high spatial resolution with medium spatial resolution is essential for a small study area and can improve accuracy assessment values. To address this study's limitation and future work, it is essential to consider other factors that impact downstream vegetation areas, such as Land Use Land Cover (LULC), soil components, wetlands, and groundwater. Climate variables do not have a significant impact, whereas other variables could have more impact on downstream vegetation area.

Abbreviations

The following abbreviations are used in this manuscript:

NDVI	Normalized Difference Vegetation Index
EWT	Equivalent Water Thickness
P	Precipitation
E	Evaporation
R	Runoff
MLC	Maximum Likelihood Classification
SPOT	Satellite Pour l'Observation de la Terre

LULC	Land Use Land Cover
GIS	Geographical Information System
TWS	Total Water Storage
GRACE	Gravity Recovery and Climate Experiment
USGS	United States Geological Survey
ERA-5	European Centre for Medium-Range Weather Forecasts Integrated Forecasting System, the fifth-generation reanalysis
GLDAS	Global Land Data Assimilation System
NIR	Near-infrared
RED	Red Band

References

1. AghaKouchak, A.; Mirchi, A.; Madani, K.; Di Baldassarre, G.; Nazemi, A.; Alborzi, A.; Anjileli, H.; Azarderakhsh, M.; Chiang, F.; Hassanzadeh, E. *Anthropogenic Drought: Definition, Challenges, and Opportunities*; Wiley Online Library: Hoboken, NJ, USA, 2021.
2. McDowell, N.; Pockman, W.T.; Allen, C.D.; Breshears, D.D.; Cobb, N.; Kolb, T.; Plaut, J.; Sperry, J.; West, A.; Williams, D.G. Mechanisms of plant survival and mortality during drought: Why do some plants survive while others succumb to drought? *New Phytol.* **2008**, *178*, 719–739. [CrossRef]
3. Jiang, M.; Tian, S.; Zheng, Z.; Zhan, Q.; He, Y. Human activity influences on vegetation cover changes in Beijing, China, from 2000 to 2015. *Remote Sens.* **2017**, *9*, 271. [CrossRef]
4. Hobbs, R.J.; Harris, J.A. Restoration ecology: Repairing the earth's ecosystems in the new millennium. *Restor. Ecol.* **2001**, *9*, 239–246. [CrossRef]
5. Soepboer, W.; Sugita, S.; Lotter, A.F. Regional vegetation-cover changes on the Swiss Plateau during the past two millennia: A pollen-based reconstruction using the REVEALS model. *Quat. Sci. Rev.* **2010**, *29*, 472–483. [CrossRef]
6. Leavesley, G.H. Modeling the effects of climate change on water resources—A review. *Clim. Chang.* **1994**, *28*, 159–177. [CrossRef]
7. Wang, J.; Rich, P.M.; Price, K.P. Temporal responses of NDVI to precipitation and temperature in the central Great Plains, USA. *Int. J. Remote Sens.* **2003**, *24*, 2345–2364. [CrossRef]
8. Nageswara Rao, P.; Shobha, S.; Ramesh, K.; Somashekhar, R. Satellite-based assessment of agricultural drought in Karnataka state. *J. Indian Soc. Remote Sens.* **2005**, *33*, 429–434. [CrossRef]
9. Bhandari, A.; Kumar, A.; Singh, G. Feature extraction using Normalized Difference Vegetation Index (NDVI): A case study of Jabalpur city. *Procedia Technol.* **2012**, *6*, 612–621. [CrossRef]
10. Gandhi, G.M.; Parthiban, S.; Thummalu, N.; Christy, A. Ndvi: Vegetation change detection using remote sensing and gis–A case study of Vellore District. *Procedia Comput. Sci.* **2015**, *57*, 1199–1210. [CrossRef]
11. Jamieson, M.A.; Trowbridge, A.M.; Raffa, K.F.; Lindroth, R.L. Consequences of climate warming and altered precipitation patterns for plant-insect and multitrophic interactions. *Plant Physiol.* **2012**, *160*, 1719–1727. [CrossRef]
12. Li, L.; Ustin, S.L.; Lay, M. Application of AVIRIS data in detection of oil-induced vegetation stress and cover change at Jornada, New Mexico. *Remote Sens. Environ.* **2005**, *94*, 1–16. [CrossRef]
13. Xu, Y.; Yang, J.; Chen, Y. NDVI-based vegetation responses to climate change in an arid area of China. *Theor. Appl. Climatol.* **2016**, *126*, 213–222. [CrossRef]
14. Lian, X.; Piao, S.; Chen, A.; Huntingford, C.; Fu, B.; Li, L.Z.; Huang, J.; Sheffield, J.; Berg, A.M.; Keenan, T.F. Multifaceted characteristics of dryland aridity changes in a warming world. *Nat. Rev. Earth Environ.* **2021**, *2*, 232–250. [CrossRef]
15. Maliva, R.; Missimer, T. *Arid Lands Water Evaluation and Management*; Springer Science & Business Media: Berlin/Heidelberg, Germany, 2012.
16. Gaur, M.K.; Squires, V.R. Geographic Extent and Characteristics of the World's Arid Zones and Their Peoples. In *Climate Variability Impacts on Land Use and Livelihoods in Drylands*; Springer: Berlin/Heidelberg, Germany, 2018; pp. 3–20.
17. Foody, G. Geographical weighting as a further refinement to regression modelling: An example focused on the NDVI–rainfall relationship. *Remote Sens. Environ.* **2003**, *88*, 283–293. [CrossRef]
18. Fayech, D.; Tarhouni, J. Climate variability and its effect on normalized difference vegetation index (NDVI) using remote sensing in semi-arid area. *Model. Earth Syst. Environ.* **2021**, *7*, 1667–1682. [CrossRef]
19. Schmidt, H.; Karnieli, A. Remote sensing of the seasonal variability of vegetation in a semi-arid environment. *J. Arid Environ.* **2000**, *45*, 43–59. [CrossRef]
20. Xie, B.; Jia, X.; Qin, Z.; Shen, J.; Chang, Q. Vegetation dynamics and climate change on the Loess Plateau, China: 1982–2011. *Reg. Environ. Chang.* **2016**, *16*, 1583–1594. [CrossRef]
21. Shi, Y.; Shen, Y.; Kang, E.; Li, D.; Ding, Y.; Zhang, G.; Hu, R. Recent and future climate change in northwest China. *Clim. Chang.* **2007**, *80*, 379–393. [CrossRef]
22. Zhou, W.; Gang, C.; Zhou, L.; Chen, Y.; Li, J.; Ju, W.; Odeh, I. Dynamic of grassland vegetation degradation and its quantitative assessment in the northwest China. *Acta Oecol.* **2014**, *55*, 86–96. [CrossRef]
23. Tong, S.; Zhang, J.; Bao, Y.; Lai, Q.; Lian, X.; Li, N.; Bao, Y. Analyzing vegetation dynamic trend on the Mongolian Plateau based on the Hurst exponent and influencing factors from 1982–2013. *J. Geogr. Sci.* **2018**, *28*, 595–610. [CrossRef]

24. Degu, A.M.; Hossain, F.; Niyogi, D.; Pielke Sr, R.; Shepherd, J.M.; Voisin, N.; Chronis, T. The influence of large dams on surrounding climate and precipitation patterns. *Geophys. Res. Lett.* **2011**, *38*, L04405. [CrossRef]
25. Zhao, Y.; Liu, S.; Shi, H. Impacts of dams and reservoirs on local climate change: A global perspective. *Environ. Res. Lett.* **2021**, *16*, 104043. [CrossRef]
26. Chen, P. *Material Science and Environmental Engineering: Proceedings of the 3rd Annual 2015 International Conference on Material Science and Environmental Engineering (ICMSEE2015, Wuhan, Hubei, China, 5–6 June 2015)*; CRC Press: Boca Raton, FL, USA, 2015.
27. Miller, N.L.; Jin, J.; Tsang, C.F. Local climate sensitivity of the Three Gorges Dam. *Geophys. Res. Lett.* **2005**, *32*, L16704. [CrossRef]
28. Wu, L.; Zhang, Q.; Jiang, Z. Three Gorges Dam affects regional precipitation. *Geophys. Res. Lett.* **2006**, *33*, L13806. [CrossRef]
29. Missimer, T.M.; Drewes, J.E.; Amy, G.; Maliva, R.G.; Keller, S. Restoration of wadi aquifers by artificial recharge with treated waste water. *Groundwater* **2012**, *50*, 514–527. [CrossRef]
30. Tarawneh, Q.Y.; Chowdhury, S. Trends of climate change in Saudi Arabia: Implications on water resources. *Climate* **2018**, *6*, 8. [CrossRef]
31. Almalki, R.; Khaki, M.; Saco, P.M.; Rodriguez, J.F. Monitoring and Mapping Vegetation Cover Changes in Arid and Semi-Arid Areas Using Remote Sensing Technology: A Review. *Remote Sens.* **2022**, *14*, 5143. [CrossRef]
32. Belal, A.-A.; El-Ramady, H.R.; Mohamed, E.S.; Saleh, A.M. Drought risk assessment using remote sensing and GIS techniques. *Arab. J. Geosci.* **2014**, *7*, 35–53. [CrossRef]
33. Ahmed, S. Assessment of urban heat islands and impact of climate change on socioeconomic over Suez Governorate using remote sensing and GIS techniques. *Egypt. J. Remote Sens. Space Sci.* **2018**, *21*, 15–25. [CrossRef]
34. Hu, M.Q.; Mao, F.; Sun, H.; Hou, Y.Y. Study of normalized difference vegetation index variation and its correlation with climate factors in the three-river-source region. *Int. J. Appl. Earth Obs. Geoinf.* **2011**, *13*, 24–33. [CrossRef]
35. Srivastava, S.; Jayaraman, V.; Nageswara Rao, P.; Manikiam, B.; Chandrasekhar, M. Interlinkages of NOAA/AVHRR derived integrated NDVI to seasonal precipitation and transpiration in dryland tropics. *Int. J. Remote Sens.* **1997**, *18*, 2931–2952. [CrossRef]
36. Ji, L.; Peters, A.J. A spatial regression procedure for evaluating the relationship between AVHRR-NDVI and climate in the northern Great Plains. *Int. J. Remote Sens.* **2004**, *25*, 297–311. [CrossRef]
37. Tangdamrongsub, N.; Han, S.-C.; Jasinski, M.F.; Šprlák, M. Quantifying water storage change and land subsidence induced by reservoir impoundment using GRACE, Landsat, and GPS data. *Remote Sens. Environ.* **2019**, *233*, 111385. [CrossRef]
38. Alshehri, F.; Mohamed, A. Analysis of Groundwater Storage Fluctuations Using GRACE and Remote Sensing Data in Wadi As-Sirhan, Northern Saudi Arabia. *Water* **2023**, *15*, 282. [CrossRef]
39. Alarifi, S.S.; Abdelkareem, M.; Abdalla, F.; Alotaibi, M. Flash Flood Hazard Mapping Using Remote Sensing and GIS Techniques in Southwestern Saudi Arabia. *Sustainability* **2022**, *14*, 14145. [CrossRef]
40. Hasanean, H.; Almazroui, M. Rainfall: Features and variations over Saudi Arabia, a review. *Climate* **2015**, *3*, 578–626. [CrossRef]
41. Zhong, L.; Ma, Y.; Hu, Z.; Fu, Y.; Hu, Y.; Wang, X.; Cheng, M.; Ge, N. Estimation of hourly land surface heat fluxes over the Tibetan Plateau by the combined use of geostationary and polar-orbiting satellites. *Atmos. Chem. Phys.* **2019**, *19*, 5529–5541. [CrossRef]
42. Xie, Z.; Huete, A.; Cleverly, J.; Phinn, S.; McDonald-Madden, E.; Cao, Y.; Qin, F. Multi-climate mode interactions drive hydrological and vegetation responses to hydroclimatic extremes in Australia. *Remote Sens. Environ.* **2019**, *231*, 111270. [CrossRef]
43. Borsa, A.A.; Agnew, D.C.; Cayan, D.R. Ongoing drought-induced uplift in the western United States. *Science* **2014**, *345*, 1587–1590. [CrossRef]
44. Otukei, J.R.; Blaschke, T. Land cover change assessment using decision trees, support vector machines and maximum likelihood classification algorithms. *Int. J. Appl. Earth Obs. Geoinf.* **2010**, *12*, S27–S31. [CrossRef]
45. Richards, J.A.; Richards, J. *Remote Sensing Digital Image Analysis*; Springer: Berlin/Heidelberg, Germany, 1999; Volume 3.
46. Mohajane, M.; Essahlaoui, A.; Oudija, F.; Hafyani, M.E.; Hmaidi, A.E.; Ouali, A.E.; Randazzo, G.; Teodoro, A.C. Land use/land cover (LULC) using landsat data series (MSS, TM, ETM+ and OLI) in Azrou Forest, in the Central Middle Atlas of Morocco. *Environments* **2018**, *5*, 131. [CrossRef]
47. Zaidi, S.M.; Akbari, A.; Abu Samah, A.; Kong, N.S.; Gisen, A.; Isabella, J. Landsat-5 Time Series Analysis for Land Use/Land Cover Change Detection Using NDVI and Semi-Supervised Classification Techniques. *Pol. J. Environ. Stud.* **2017**, *26*, 2833–2840. [CrossRef] [PubMed]
48. Munier, S.; Aires, F.; Schlaffer, S.; Prigent, C.; Papa, F.; Maisongrande, P.; Pan, M. Combining data sets of satellite-retrieved products for basin-scale water balance study: 2. Evaluation on the Mississippi Basin and closure correction model. *J. Geophys. Res. Atmos.* **2014**, *119*, 12–100. [CrossRef]
49. Sheffield, J.; Ferguson, C.R.; Troy, T.J.; Wood, E.F.; McCabe, M.F. Closing the terrestrial water budget from satellite remote sensing. *Geophys. Res. Lett.* **2009**, *36*, L07403. [CrossRef]
50. Tranmer, M.; Elliot, M. Multiple linear regression. *Cathie Marsh Cent. Census Surv. Res.* **2008**, *5*, 1–5.
51. Morgounov, A.; Abubakr, M.; Alhendi, A.; Alkhatran, A.; Alhuwaymil, H.; Ghosh, K. Agroclimatic Zones and Cropping Systems in the Southwestern Regions of the Kingdom of Saudi Arabia: Characterization, Classification and Improvement Potential. *Crops* **2022**, *2*, 186–201. [CrossRef]
52. Guarino, L.; Al-Juwaeid, A.A. Wheat Collecting in Saudi Arabia. In *2 Food and Agriculture Organization of the United Nations@ Organisation Des Nations Unies Pour L'alimentation Et L'agriculture Organizacion De Las Naciones Unidas Para La Agricultura Y La Alimentacion*; Food and Agriculture Organization: Rome, Italy, 1990; Volume 36.

53. Congalton, R.G. A review of assessing the accuracy of classifications of remotely sensed data. *Remote Sens. Environ.* **1991**, *37*, 35–46. [CrossRef]
54. Dehwah, A.H.; Al-Mashharawi, S.; Missimer, T.M. Mapping to assess feasibility of using subsurface intakes for SWRO, Red Sea coast of Saudi Arabia. *Desalination Water Treat.* **2014**, *52*, 2351–2361. [CrossRef]
55. Lopez, O.; Stenchikov, G.; Missimer, T. Water management during climate change using aquifer storage and recovery of stormwater in a dunefield in western Saudi Arabia. *Environ. Res. Lett.* **2014**, *9*, 075008. [CrossRef]
56. Almazroui, M.; Nazrul Islam, M.; Athar, H.; Jones, P.; Rahman, M.A. Recent climate change in the Arabian Peninsula: Annual rainfall and temperature analysis of Saudi Arabia for 1978–2009. *Int. J. Climatol.* **2012**, *32*, 953–966. [CrossRef]
57. Almazroui, M. Changes in temperature trends and extremes over Saudi Arabia for the period 1978–2019. *Adv. Meteorol.* **2020**, *2020*, 8828421. [CrossRef]
58. Sehler, R.; Li, J.; Reager, J.; Ye, H. Investigating relationship between soil moisture and precipitation globally using remote sensing observations. *J. Contemp. Water Res. Educ.* **2019**, *168*, 106–118. [CrossRef]
59. Guillod, B.P.; Orlowsky, B.; Miralles, D.G.; Teuling, A.J.; Seneviratne, S.I. Reconciling spatial and temporal soil moisture effects on afternoon rainfall. *Nat. Commun.* **2015**, *6*, 6443. [CrossRef]
60. Alrwis, K.N.; Ghanem, A.M.; Alnashwan, O.S.; Al Duwais, A.A.M.; Alaagib, S.A.B.; Aldawdahi, N.M. Measuring the impact of water scarcity on agricultural economic development in Saudi Arabia. *Saudi J. Biol. Sci.* **2021**, *28*, 191–195. [CrossRef]
61. Şen, Z.; Al Alsheikh, A.; Al-Turbak, A.; Al-Bassam, A.; Al-Dakheel, A. Climate change impact and runoff harvesting in arid regions. *Arab. J. Geosci.* **2013**, *6*, 287–295. [CrossRef]
62. Almazroui, M. Rainfall trends and extremes in Saudi Arabia in recent decades. *Atmosphere* **2020**, *11*, 964. [CrossRef]
63. Liu, B.; Zou, X.; Yi, S.; Sneeuw, N.; Cai, J.; Li, J. Identifying and separating climate-and human-driven water storage anomalies using GRACE satellite data. *Remote Sens. Environ.* **2021**, *263*, 112559. [CrossRef]
64. Yang, X.-D.; Ali, A.; Xu, Y.-L.; Jiang, L.-M.; Lv, G.-H. Soil moisture and salinity as main drivers of soil respiration across natural xeromorphic vegetation and agricultural lands in an arid desert region. *Catena* **2019**, *177*, 126–133. [CrossRef]
65. Sallam, A.; Bader Alharbi, A.; Usman, A.R.; Hussain, Q.; Ok, Y.S.; Alshayaa, M.; Al-Wabel, M. Environmental consequences of dam construction: A case study from Saudi Arabia. *Arab. J. Geosci.* **2018**, *11*, 47. [CrossRef]
66. Khalifa, H.; Moussa, H. Soil and agriculture after the Aswan High Dam. In *Irrigated Agriculture in Egypt: Past, Present and Future*; Spinger: Berlin/Heidelberg, Germany, 2017; pp. 81–124; ISBN 978-3-319-30216-4. [CrossRef]
67. Chowdhury, S.; Al-Zahrani, M. Reuse of treated wastewater in Saudi Arabia: An assessment framework. *J. Water Reuse Desalination* **2013**, *3*, 297–314. [CrossRef]
68. Abderrahman, W.; Al-Harazin, I. *Assessment of Climate Changes on Water Resources in the Kingdom of Saudi Arabia, GCC Environment and Sustainable Development Symposium, 28–30 January 2008, Dhahran, Saudi Arabia*; Wiley Online Library: Hoboken, NJ, USA, 2008; pp. D-1-1–D-1-13.
69. Mallick, J.; AlMesfer, M.K.; Singh, V.P.; Falqi, I.I.; Singh, C.K.; Alsubih, M.; Kahla, N.B. Evaluating the NDVI–rainfall relationship in Bisha watershed, Saudi Arabia using non-stationary modeling technique. *Atmosphere* **2021**, *12*, 593. [CrossRef]
70. IWMI. *Strategy 2014–2018—Solutions for a Water-Secure World*; International Water Management Institute Colombo: Battaramulla, Sri Lanka, 2014.
71. Tangdamrongsub, N.; Han, S.-C.; Decker, M.; Yeo, I.-Y.; Kim, H. On the use of the GRACE normal equation of inter-satellite tracking data for estimation of soil moisture and groundwater in Australia. *Hydrol. Earth Syst. Sci.* **2018**, *22*, 1811–1829. [CrossRef]
72. Pan, Y.; Zhang, C.; Gong, H.; Yeh, P.J.F.; Shen, Y.; Guo, Y.; Huang, Z.; Li, X. Detection of human-induced evapotranspiration using GRACE satellite observations in the Haihe River basin of China. *Geophys. Res. Lett.* **2017**, *44*, 190–199. [CrossRef]
73. Almalki, R.; Piwowar, J.; Siemer, J. Geographical considerations in site selection for small modular reactors in Saskatchewan. *Geosciences* **2019**, *9*, 402. [CrossRef]